

# About the Chemical Enrichment of $\omega$ Centauri (and dSphs central regions)

A. Marcolini<sup>1</sup>, A. Sollima<sup>2</sup>, A. D'Ercole<sup>3</sup>, B.K. Gibson<sup>1</sup> and F.R. Ferraro<sup>2</sup>.

(<sup>1</sup> University of Central Lancashire; <sup>2</sup> Bologna University; <sup>3</sup> Bologna Observatory)

**Abstract:** We present a hydrodynamical and chemical model for the globular cluster  $\omega$  Centauri assuming it as the remnant of an ancient dwarf spheroidal galaxy (dSph) swallowed by our Galaxy  $\sim 10$  Gyr ago.

**1:** To understand the chemical enrichment of  $\omega$  Cen it is necessary to recognize its star formation history (SFH) and the role of supernovae (SNe) feedback on its evolution. Marcolini et al. 2006 ran a number of three-dimensional hydrodynamical simulations to study the evolution of isolated dSphs, objects similar to that from which  $\omega$  Cen possibly originated. The authors assumed a prolonged intermittent SFH (see left-lower panel in Fig. 2), paying attention to the influence of both SNe Ia and SNe II on the chemical content of the new forming stars. After each starburst, SNe II start to explode near the galactic centre, where their remnants overlap forming a single cavity composed of a network of tunnels filled by hot rarefied gas (see Fig. 1). Most of the interstellar medium (ISM) is pushed outward, toward the edge of the cavity. Once the SNe II stop to explode (30 Myr after each starburst episode) the global cavity collapses and the ISM goes back into the potential well, giving rise to a new starburst. **Given their lower rate, SNe Ia do not significantly affect the general hydrodynamical behaviour of the ISM, but their role is relevant for the chemical evolution of the forming stars.** Because of their longer timescales, SNe Ia progenitors produced in previous starbursts continue to explode during the quiescent periods, when the gas has settled back to the central region. The higher ambient gas density leads SNe Ia remnants to be located quite apart one from another.

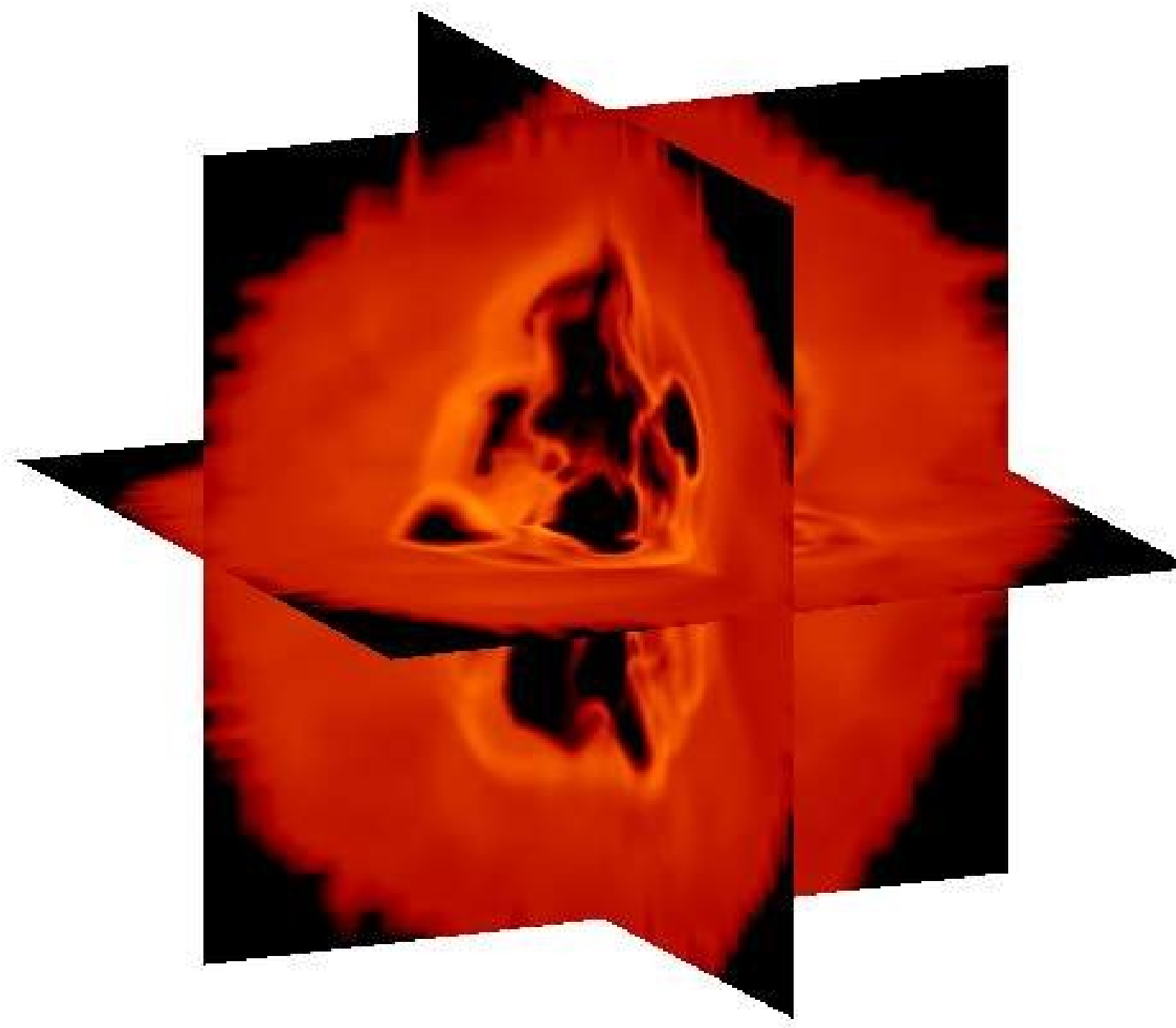


Fig. 1: density distribution of the interstellar medium in three different orthogonal planes after a time interval of  $\sim 20$  Myr from the occurrence of the third instantaneous burst.

**2:** As a consequence of the inhomogeneous SNIa pollution, stars forming in the regions occupied by SN Ia remnants (hereafter referred to as "SNe Ia pockets") have lower  $[\alpha/\text{Fe}]$  ratios and higher  $[\text{Fe}/\text{H}]$  ratios than those formed elsewhere. This effect is particularly important for the chemical evolution of the central region, where the SN Ia rate is larger and where SN Ia pockets formed in the outer zones are dragged by the gas flow during the re-collapse phases. The upper panels in Fig. 2 show the  $[\text{Fe}/\text{H}]$  distribution of the long-lived stars for the dSph model and the  $\omega$  Cen model (i.e. the dSph central region). For the latter, SF is supposed to drop rapidly after  $\sim 1$  Gyr (see right-lower panel in Fig. 2) due to the interaction with the Milky Way. **While the distribution shown in the left-upper panel is very similar to those found in some dSphs (e.g. Bellazzini et al. 2002; Koch et al. 2006), the profile referring to the central region clearly shows a bimodal structure similar to that observed in  $\omega$  Cen (e.g. Norris et al. 1996; Suntzeff et al. 1996), with a maximum at  $[\text{Fe}/\text{H}] \sim -1.6$  and a secondary peak at  $[\text{Fe}/\text{H}] \sim -1.3$  accounting for the  $\sim 25\%$  of the entire cluster stellar content.** The different shape of the distribution is due to the higher presence of SN Ia pockets in this region. The middle panels in Fig. 2 show the  $[\alpha/\text{Fe}]$ - $[\text{Fe}/\text{H}]$  diagram for 1000 sampled stars for the two models. Again, because of the SN Ia contribution, some of the Fe-rich stars ( $[\text{Fe}/\text{H}] > -1.5$ ) are, as expected,  $\alpha$ -depleted and their number is much higher in the central region.

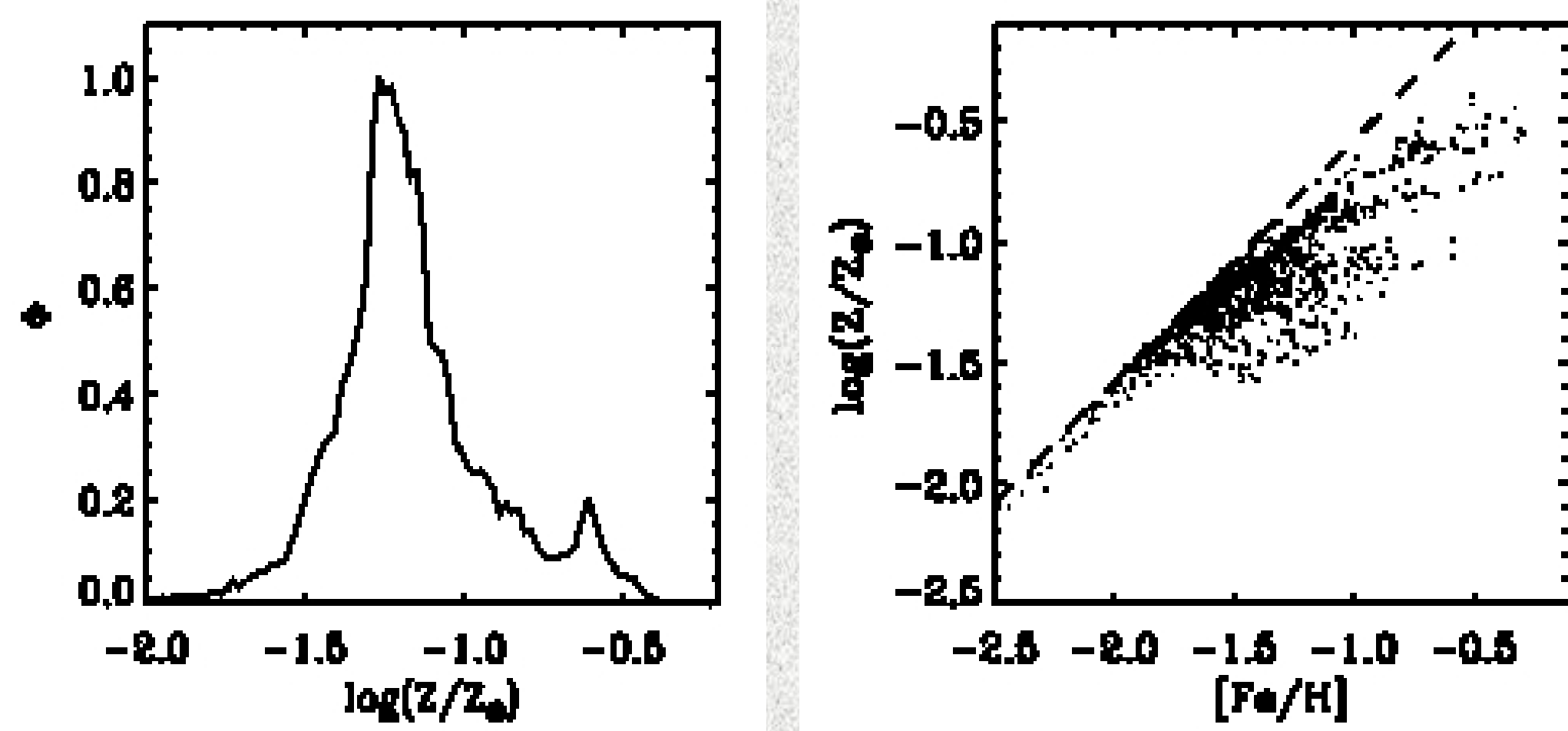


Fig. 3: left panel:  $\log(Z/Z_{\odot})$  stellar distribution. Right panel:  $\log(Z/Z_{\odot})$ - $[\text{Fe}/\text{H}]$  diagram of 1000 stars sampled in the central region ( $\omega$  Cen model).

**3:** We emphasize the difference between the pollution of iron and that of metals as a whole. It is known that the ratio between the iron mass and the mass of all the metals is rather different in the ejecta of the two types of SNe. Thus, when the contribution of the SNe Ia to the ISM pollution becomes relevant, the metal mass fraction Z is not linearly proportional to the  $[\text{Fe}/\text{H}]$  content. The Z distribution for the long lived stars is plotted in Fig. 3 (left panel). The bimodal structure near the main peak of the  $[\text{Fe}/\text{H}]$  distribution is now absent. In fact, after  $\sim 1$  Gyr for example, the number of SNe Ia that occurred account for  $\sim 20\%$  of the iron content and only for 2% of the produced metal mass. Therefore, in the regions polluted by SNe Ia, the  $[\text{Fe}/\text{H}]$  ratio drastically increases, but the metal mass fraction Z remains basically unaffected.

This effect is particularly evident in Fig. 4 (right panel) where the  $\log(Z/Z_{\odot})$ - $[\text{Fe}/\text{H}]$  diagram for 1000 sampled stars is shown. The dashed line represents the  $\log(Z/Z_{\odot})$ - $[\text{Fe}/\text{H}]$  relation for stars formed in regions enriched only by SNe II. It is evident that a non negligible number of stars do not follow this relation. **As a consequence in the central regions, Fe-rich ( $[\text{Fe}/\text{H}] > -1.4$ ) and Fe-poor ( $[\text{Fe}/\text{H}] < -1.4$ ) stars may have nearly the same metal mass fraction Z.**

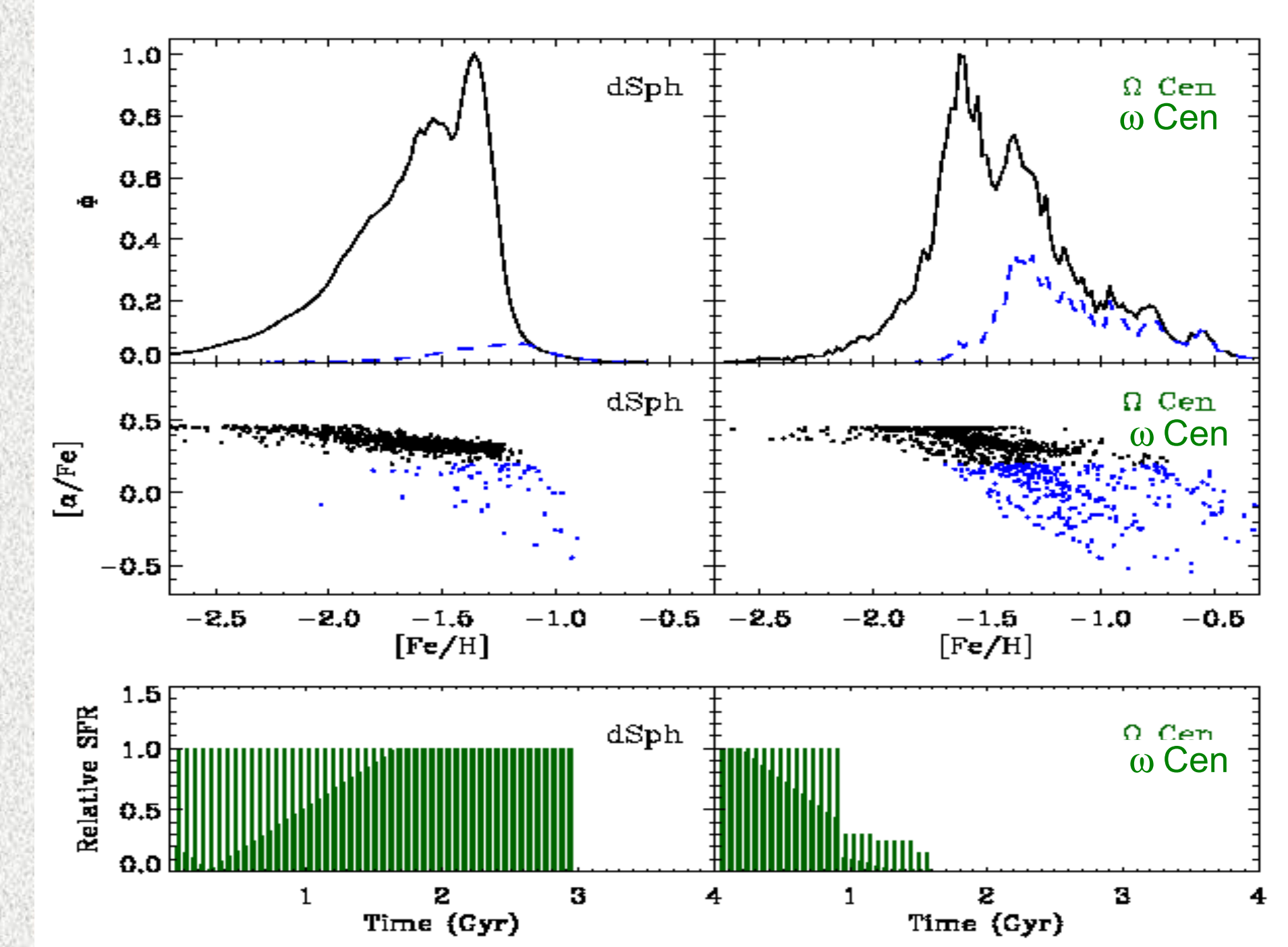


Fig. 2: upper panels:  $[\text{Fe}/\text{H}]$  distribution of the stars formed in a volume resembling the whole dSph (left panel) and in a volume resembling its nucleus ( $R < 90$  pc, right panel). Middle panels:  $[\alpha/\text{Fe}]$  against the  $[\text{Fe}/\text{H}]$  of 1000 sampled stars in the two region defined above. Lower panels: temporal profile of the assumed star formation rate for the dSph model (left panel) and the  $\omega$  Cen model (right panel). Blue symbols refer to stars with  $[\alpha/\text{Fe}] < 0.2$ .

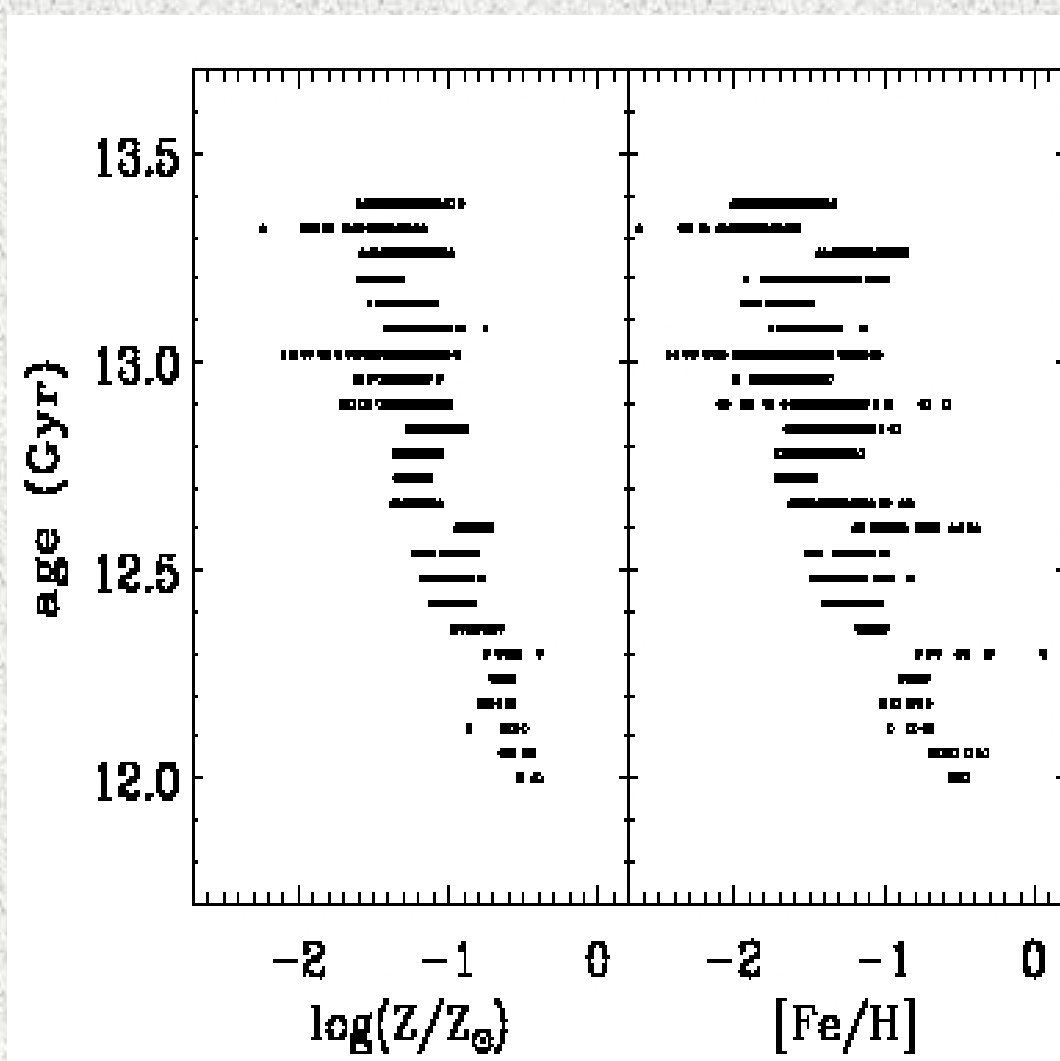


Fig. 4: Age-metallicity distributions of 1000 sampled stars: note the metallicity spread among coeval stars.

**4:** In the central region of our model the metallicity increases with time even if a large spread is always present in agreement with the most recent determinations (e.g. Hilker et al. 2004; Stanford et al. 2006). Note that the spread is more evident in the  $[\text{Fe}/\text{H}]$  distribution, rather than in the Z one, because of the stronger influence of the inhomogeneous SNIa enrichment on the Fe abundance. **We find that the entire metal enrichment process of  $\omega$  Cen takes place during  $\sim 2$  Gyr.**

**5:** Most of the evidences gathered in the past on the metallicity spread, the presence of multiple populations and the possible helium enhancement in  $\omega$  Cen have been deduced from the peculiar morphology of different sequences in the CMD. It is interesting to check how our models compare with the most recent and accurate observational data. As a first step, in order to simulate the morphology of the CMD we used the evolutionary tracks by Cassisi et al. (2004) and Pietrinferni et al. (2006) calculated for two different  $\alpha$ -enhancement levels ( $[\alpha/\text{Fe}] = 0.0$  and  $[\alpha/\text{Fe}] = 0.4$ ). In Fig. 5 the color distribution of RGB stars at two different magnitude levels is shown for both the simulated ( $\omega$  Cen model) and the observed (Sollima et al. 2005) CMD in the (V, B-V) plane. **The color distribution of the RGB of  $\omega$  Cen is well reproduced. The most metal-rich anomalous component (RGB-a,  $[\text{Fe}/\text{H}] \sim -0.6$ ), well distinguishable in the red part of the CMD of Sollima et al. 2005, is less defined in our model (although still present).** A behavior similar to that observed in Fig. 5 is also present in Fig. 6, where our  $\omega$  Cen model is compared with the ACS CMD by Ferraro et al. (2004) in the sub-giant branch (SGB) region. **As can be noted, the observed magnitude spread of the upper part of the SGB, as well as the presence of the anomalous SGB (SGB-a), are accounted for. According to our model, stars lying along this sequence have a high iron content ( $[\text{Fe}/\text{H}] \sim -0.6$ ).** Indeed, this anomalous metal-rich population appears to form in the last 600 Myr of evolution of  $\omega$  Cen, after 1 Gyr from the beginning of the SF.

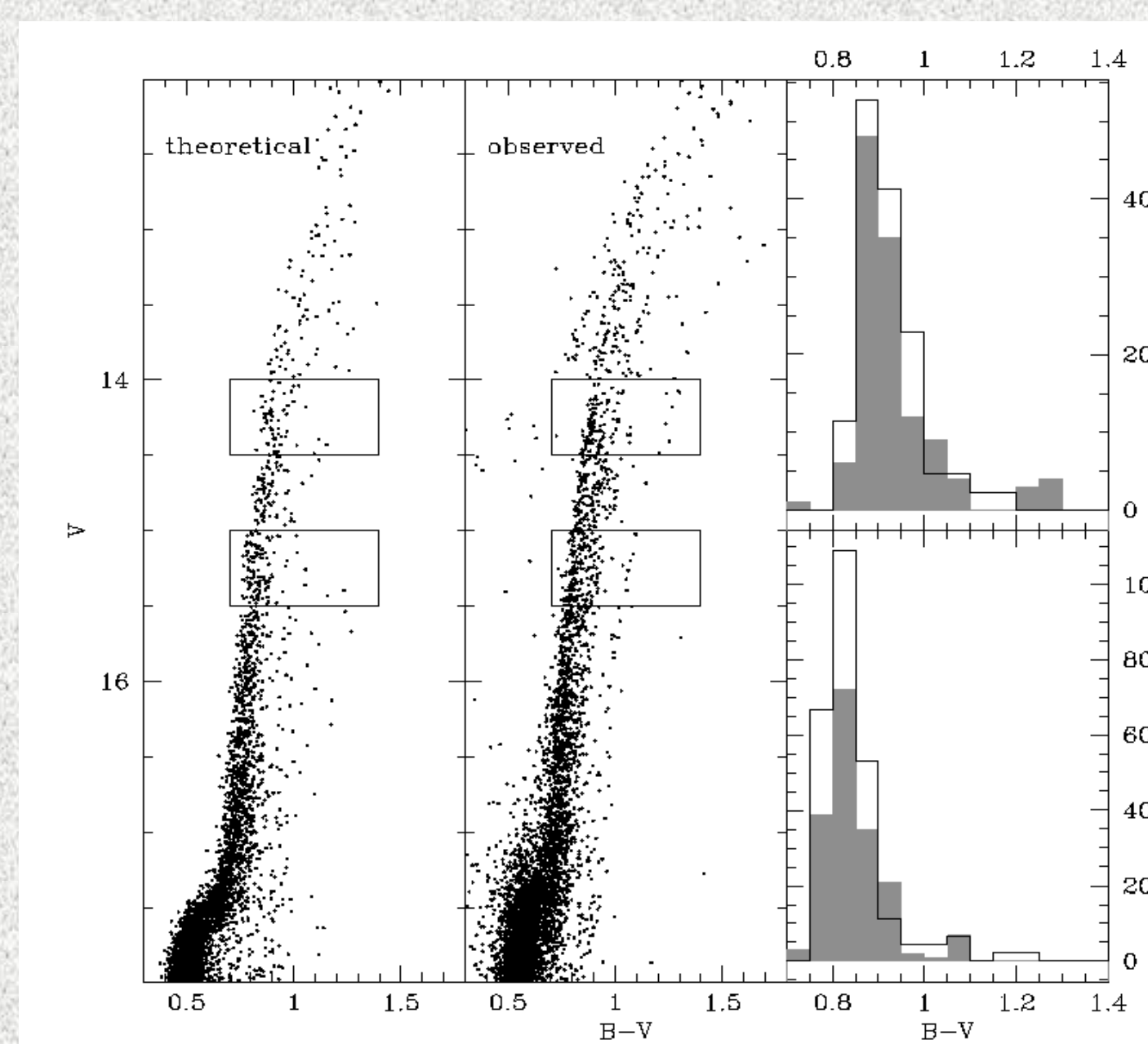


Fig. 5: Comparison between the simulated (grey histograms) and the observed (from Sollima et al. 2005) (V; B-V) CMD of  $\omega$  Cen

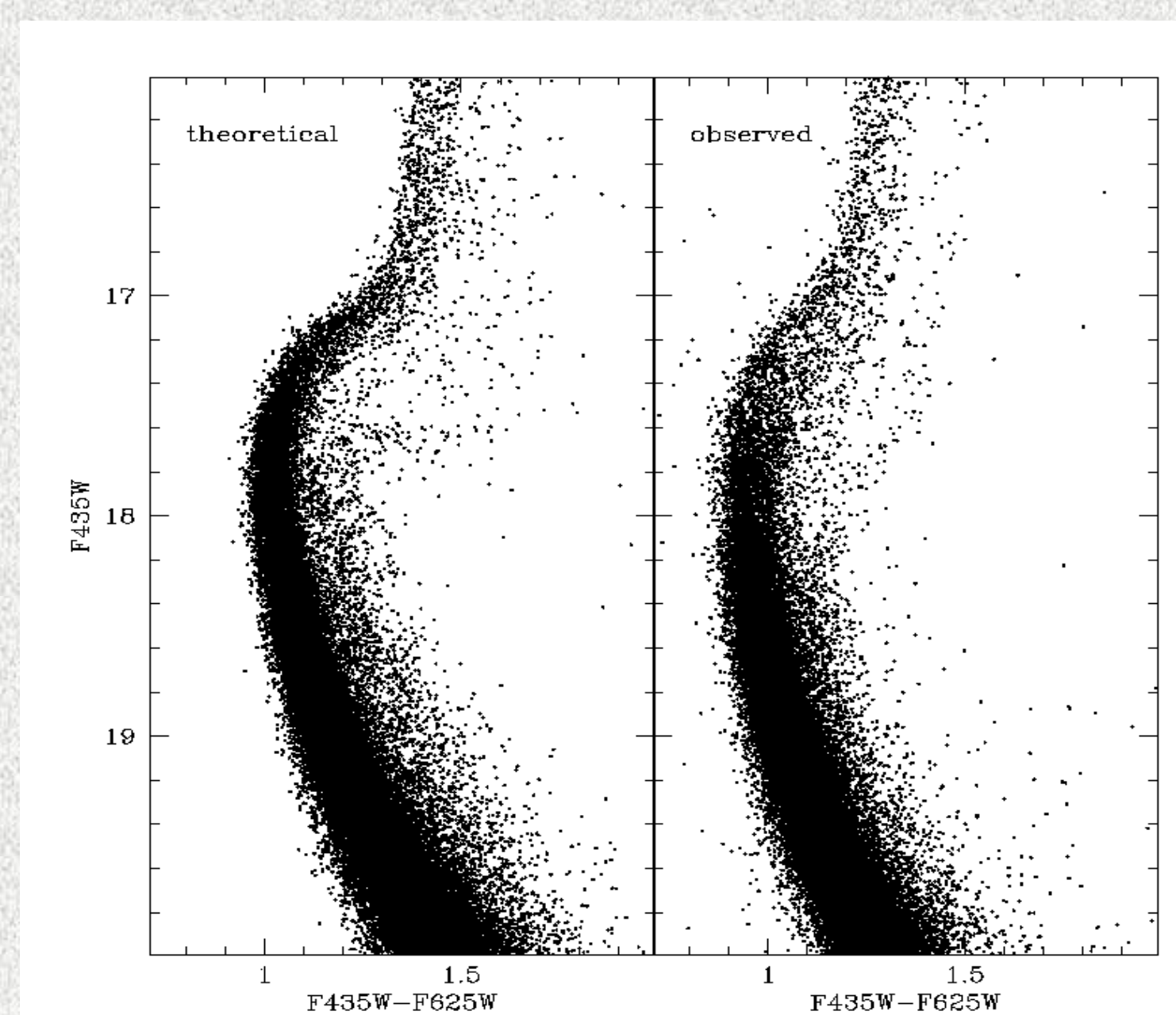


Fig. 6: Comparison between the simulated (left panel) and observed (from Ferraro et al. 2001) (F625W; F435W-F625W) CMD of  $\omega$  Cen.

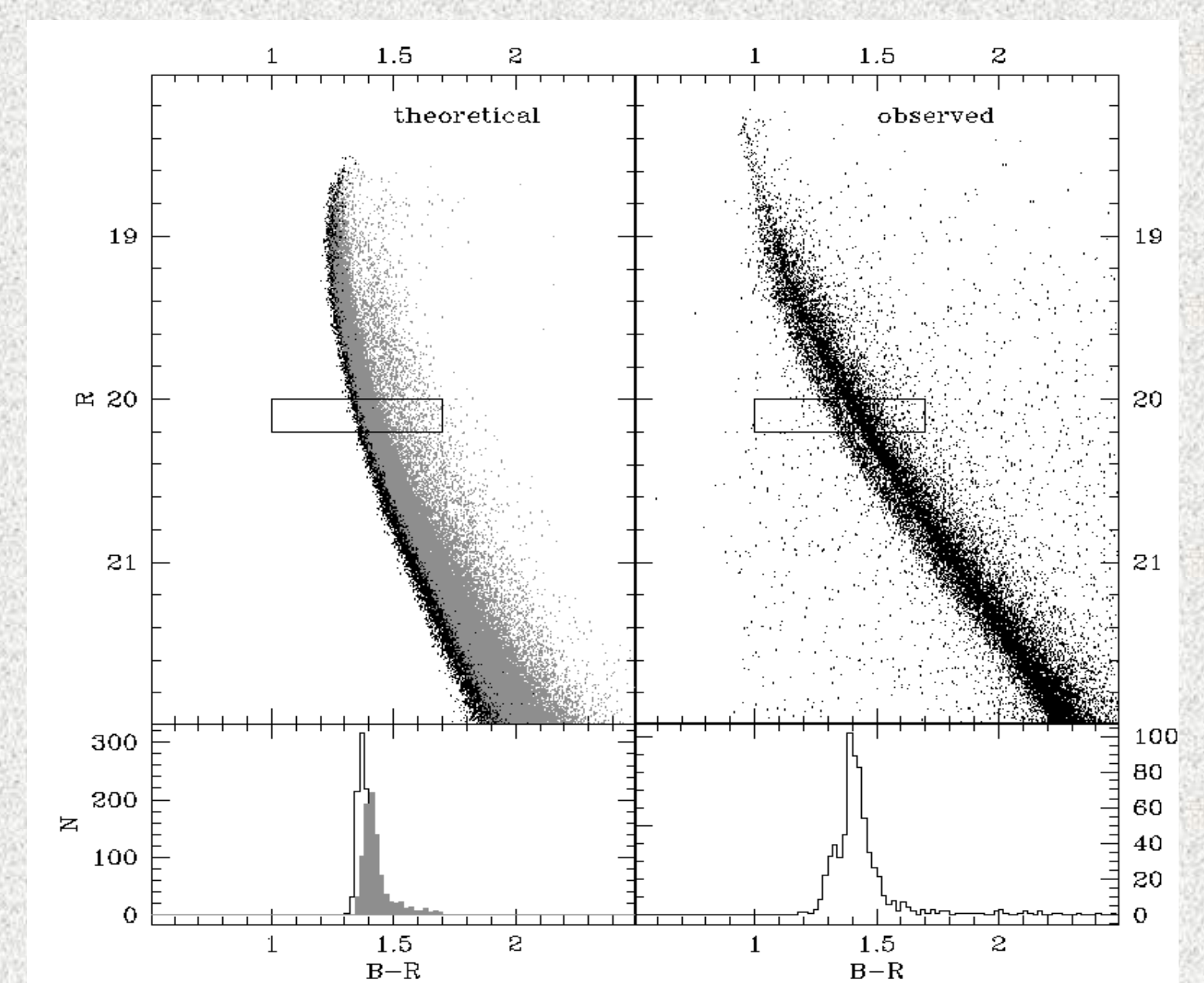


Fig. 7: Comparison between the simulated (left panels) and observed (from Sollima et al. 2007) (R; B-R) CMD. Grey points in the left panel marks stars with  $[\text{Fe}/\text{H}] > -1.4$ .

Finally, in Fig. 7 we compare our model with the CMD obtained by Sollima et al. 2005 from deep FORS1 observations of the MS of  $\omega$  Cen. Fe-rich stars ( $[\text{Fe}/\text{H}] > -1.4$ ) are marked as grey points in the synthetic CMD. In the bottom panels the color distributions of Fe-poor ( $[\text{Fe}/\text{H}] < -1.4$ ) and Fe-rich ( $[\text{Fe}/\text{H}] > -1.4$ ) stars in the simulated CMD and of observed stars are shown. **As can be noted, we fail in reproducing the double main sequence, but Fe-rich stars are mostly located in the same region of the other Fe-poor stars as expected for two population with similar distributions of Z.** Although our model fails to reproduce the MS morphology of  $\omega$  Cen, the lower mean  $\alpha$ -elements abundance predicted for the Fe-rich group of stars tends to reduce the color distance between blue MS and red MS.